Geometrical Improvement of a Noninvasive Core Temperature Thermometer based on Numeric Modeling and Experiment Validation

Ming Huang[1], Toshiyo Tamura[2], Wenxi Chen[3], Kei-ichiro Kitamura[4],
Tetsu Nemoto[4] and Shigehiko Kanaya[5]

[1]*Computational Systems Biology Lab, Graduate School of Information Science,*
Nara Institute of Science and Technology, 8916-5 Takayamacho, 630-0192, Ikoma, Nara, Japan
[2]*Department of Biological Engineering, Osaka Electro-Communication University, 18-8 Hatcho,*
572-8530, Neyagawa, Osaka, Japan
[3]*Biomedical Information Technology Lab, the University of Aizu, Tsuruga, Ikki-machi,*
965-8580, Aizu-wakamatsu, Fukushima, Japan
[4]*Department of Laboratory Science, Kanazawa University, 920-0942, Kanazawa Ishikawa, Japan*
[5]*Computational Systems Biology Lab, Graduate School of Information Science,*
Nara Institute of Science and Technology, 8916-5 Takayamacho, 630-0192, Ikoma, Nara, Japan

Abstract: This paper describes the improvement of a transcutaneous core temperature thermometer by modifying the configuration, in terms of height and radius, of the thermometer using the so-called dual-heat-flux (DHF) method. The motivation of these modifications is to decrease the volume of the thermometer so as to reduce the transverse heat flow inside, in other words, to preserve the underlying assumption of the DHF method that heat flows from the inner part of human body through skin onto the thermometer longitudinally. The modification's effect is evaluated by both numeric modeling based on finite element method and experiment. The results of simulations and experiments show that a lower-in-height and larger-in-radius configuration will improve the accuracy of the thermometer. Prototypes of 22.0 mm radius can attain satisfactory accuracy with error less than 0.5 °C when heights are 8.0 mm or less.

1 INTRODUCTION

Core temperature is one of the vital signs of human body and its noninvasive monitoring is valuable in both clinical aspect and daily healthcare aspect. In order to lower the probability of developing complications after surgeries, the National Institute for Health and Clinical Excellence (NICE) has issued guidance to the NHS in England and Wales to prevent hypothermia during perioperative period (NICE, 2008). However, it is acknowledged that the three standard measurement sites of pulmonary artery, nasopharynx and distal esophagus are difficult to access during the perioperative period. A clinical trial applying a transcutaneous thermometer adopting the so-called double-sensor (DS) method as an alternative to the invasive core temperature monitoring has been carried out (Kimberger et al.,

2009).

As one of the major endogenous biorhythms, the rhythm of core temperature plays a major role at the treating of sleep disorder as an important criterion of the circadian phase, because that the core temperature rhythm and the sleep/wake rhythm are closely related (Bjoryatn and Pallesen, 2009). Such kind of studies will benefit a lot from a reliable technique that is able to monitor the core temperature continuously (Baehr et al., 2000).

To meet the requirement of long-term and noninvasive measurement needs, tradeoff among the measurement accuracy, response time and safety should be made. This characteristic excludes the means such as tympanic infrared thermometer or magnetic resonance temperature mapping. A feasible choice is to use the skin-contacting temperature sensors and thermal physical principles to estimate the core temperature, which the existing

zero-heat-flux (ZHF) method (Fox and Solman, 1971), DS method (Gunga et al., 2008) and the dual-heat-flux (DHF) method (Kitamura et al., 2009) are attributed to.

Of the three said methods , ZHF is greatly limited by its adoption of heater. As for the other two methods, we have to consider the blood perfusion in the skin and subcutaneous tissue, which makes the heat conductivity in the corresponding tissues change greatly even for the same individual. This problem is tactfully dodged by DHF method.

However, the underlying assumption of DHF method that the heat flow from the inner body through the skin and subcutaneous tissue onto the thermometer longitudinally is somewhat diverging from the practical situation. The thermometer is conducting heat exchange with the ambient environment through convection and radiation. The effect of convection can be greatly moderated with proper clothing during measurement whereas the radiation can't be ignored. The insulator, featured with a relative higher emissivity, consists of the peripheral boundary of the thermometer. Thus a lower height and larger radius design may help to suppress the transverse heat flow so as to improve the accuracy.

In this study, we validated the geometrical improvement through simulation, and the effect of the geometrical modification by practical experiments with our experimental system.

This paper can be divided into two parts. The first part is to examine the effect of the geometrical modification on a physiological significant temperature range (36.0-38.0 °C) by a 3D modeling based on finite element method (FEM). The second part is to fabricate the thermometer's prototypes according to the simulation results, to construct the experimental system and finally to validate the effects of the geometrical improvement.

2 METHOD

2.1 The DHF Method

DHF method uses at least four temperature sensors inlaid inside the DHF thermometer to calculate the core temperature. Elucidation can be made based on following formulas and Fig. 1.

There is temperature difference between the deep body part and the skin surface. If we assume that the inner boundary of skin is of the same temperature with the deep body part, heat flow from inner part to skin surface will arise and then stream into the

thermometer as shown in Figure 1. Considering that heat flow from deep body part into the thermometer is the same, two equations below can be acquired by Fourier law.

$$(T_d - T_1)/R_s = (T_1 - T_3)/R_1, \quad (1)$$

$$\text{and } (T_d - T_2)/R_s = (T_2 - T_4)/R_2, \quad (2)$$

where T_d is the temperature of the inner boundary of skin, i.e., the core temperature, while T_1, T_2 is skin temperature measured by cutaneous temperature sensors inside the thermometer and T_3, T_4 are the temperature measured by the other two sensors. R_s is the heat resistance of the skin, R_1 and R_2 are the heat resistance of the two heat path inside the thermometer. According to (1), (2), T_d then can be expressed as

$$T_d = T_1 + \frac{(T_1-T_2)(T_1-T_3)}{\alpha(T_2-T_4)-(T_1-T_2)}, \quad (3)$$

Where $\alpha = R_1/R_2$ and can be represented with the ratio of length of the two concentric cylinders constructing the thermometer.

2.2 3D Modeling based on FEM

In this paper, we only carried out the stationary study of the 3D model, in other words, the whole model was assumed to be at a heat equilibrium state. It was used to mimicking the situation when the reading of the thermometer becomes stable. We also set the related thermophysical properties of each component in the model to be isotropic.

Hence, the well-acknowledged mathematical description of bioheat transfers: Pennes equation could be simplified as (4), where ω_b ρ_b, c_b, k, and q_m are perfusion rate ($m^3/m^3 \cdot s$), density (kg/m^3) specific heat ($J/kg \cdot °C$) of blood, thermal conductivity ($W/m \cdot °C$), and rate of metabolic heat generation. T is the local temperature and T_b is the temperature of blood. What is more, because we used this model to simulate the situation when the thermometer was applied to a rubber sheet that no extra heat generated inside, the second and the third terms of the equation could be eliminated.

$$0 = \nabla \cdot [k\nabla T(X)] + \omega_b\rho_b c_b(T_b - T(X)) \\ + q_m(X). \quad (4)$$

The heat exchange between the thermometer/tissues and the ambient environment was described by radiation only because that the effect of convection can be greatly mitigated by proper clothing. Hence, the boundary condition of the thermometer and the cutaneous surface is:

Table 1: Related thermophysical properties of the materials used in simulations.

Component	Conductivity (W/m·°C)	Density (kg/m³)	Specific heat (J/kg·°C)	Emissivity
Skin	0.17	1100	3500	0.98
rubber	0.06	180	2010	0.95
aluminum	400	8700	385	0.05

$$-\vec{\boldsymbol{n}} \cdot [-k(\boldsymbol{X})\nabla T(\boldsymbol{X})] = \varepsilon\sigma\left(T_{\mathrm{amb}}^4 - T_s{}^4(\boldsymbol{X})\right) \qquad (5)$$

T_{amb} and T_{s} is the ambient temperature (°C) and temperature on boundaries, respectively, σ is the Stefan–Boltzmann constant, and ε is the emissivity of material. FEM model was constructed and analyzed by COMSOL Multiphysics software (COMSOL Inc., Sweden). In this model, lower boundary of skin was considered to be of the same temperature as the core temperature, while the peripheral boundary of the skin was assumed as heat insulation. Details about this mathematical description and the underlying deduction of the DHF method can be found in (Huang and Chen, 2010) and (Kitamura, et al., 2010).

In numeric study aspect, we constructed a series of thermometer of 4 different heights ($\{h_1, h_2\}$ = {4.5, 3.0} {8.0, 5.0}, {15.0, 9.0}, {29.0, 17.0} mm) and 4 different radii ($\{\varphi_1, \varphi_2$ = {11.0, 5.5}, {22.0, 11.0}, {33.0, 16.5} {44.0, 22.0} mm}, thus a total of 16 combinations, that is 16 different configurations were used. Cross-section view of the thermometer and details of its configuration are illustrated in Figure 1.
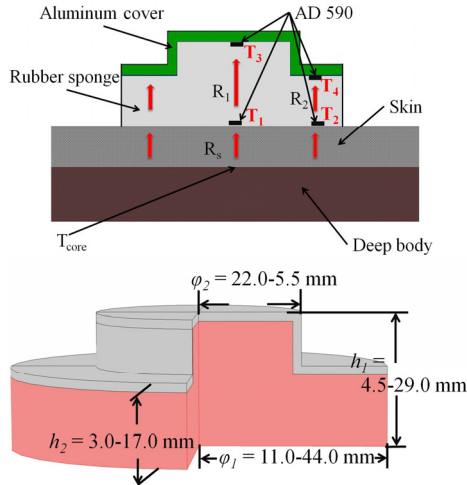

Figure 1: Upper: The illustration of the two-layer structure and the arrangement of the four temperature sensors (AD 590, Analog, 2-pin style). It is supposed that the heat from deep body part flows as the arrow's indicating and no transverse heat flow arises in the skin and the thermometer. Lower: The cross-section view of the thermometer. The thickness of the top aluminum cover is 1 mm.

With this model, we simulated the situation where the thermometer is applied to skin surface when the temperature at the bottom of skin (rubber sheet) is 36.0, 37.0 and 38.0 °C respectively, while the ambient temperature is 28.0 °C.

2.3 Prototypes and Experimental System

We fabricated a series of prototypes based on the simulations results, whose heights are different while radii are the same (22.0 mm). Because that clumsy volume is a negative factor for the universality for a transcutaneous thermometer, only the height was changed. We would only consider changing the radius of the thermometer if acceptable accuracy can't be obtained with present radius. In this paper, we illustrate the results of two prototypes, {8.0, 5.0} mm and {15.0, 9.0} mm (Figure 2). The higher one is of similar configuration with the initial prototype proposed by Kitamura et al. while the lower one is the thinnest one fabricated so far. It is reported that a thicker geometry is a negative factor for the accuracy (Huang et al., 2013). Hence, these two kinds of prototype can show the improvement based on height modification.

Figure 2: Front view of the two prototypes. Radii of the two prototypes are 22.0 mm, while heights are {15.0, 9.0} and {8.0, 5.0} mm, respectively.

The experimental system was constructed to mimic the core temperature measurement carried out on skin noninvasively, thereafter to acquire, store and process the data of those experiments.

The body-mimicking module comprises of a thermostatic water bath (± 0.1 °C systematic error) stabilizing the temperature of water and a skin-mimicking 10.0 mm neutral rubber sheet.

The data acquired by the 4 temperature sensors,

which were used to calculate the estimate of core temperature, was streamed into PC for data processing, visualizing and storage on LabVIEW platform. The program of LabVIEW was organized to suppress the measurement noise. As for the data processing in the system, the DAQ sampled temperature values from the 4 sensors, then a median filter, which performs median filtering for every 100 measurements for real-time data acquisition, was adopted in LabVIEW platform (by the function named PtByPt median filter) to acquire measurements in real time with 1 Hz sampling rate and write into a spreadsheet. This routine enables the automatic and dynamic tracing of the thermal physical evolution of the system.
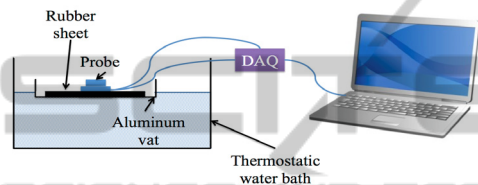

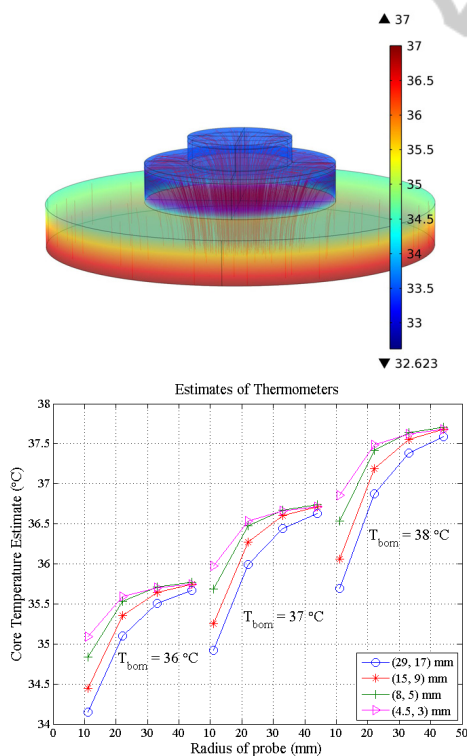Figure 3: The schema of the experimental system.

Figure 4: Upper: An image of temperature distribution and heat flow inside the prototype. Lower: Results of the simulations. X-axis is the radius of the thermometer; Y-axis is the estimates of thermometers.

With the said prototypes and experimental system, we carried out experiments in a laboratory environment, where the ambient temperature was 28.0 ± 0.5 °C. The prototypes went through tests 5 times for each condition that the bottom of the rubber sheet was regulated at 36.0, 37.0 and 38.0 °C respectively.

3 RESULTS

With the model of FEM, temperature distribution and heat flow condition corresponding to specified condition (upper figure in Figure 4) can be attained. The results of the numerical study were summarized into the lower figure in Figure 4. 3 clusters of curves mark the estimates of each configuration under different core temperature condition.

Each of the temperature situations shows similar trend. We should also notice that the latitudinal factor is more effective than the longitudinal factor in terms of accuracy.

The results of the experiments are tabulated in Table 1. In order to make an easier comparison, the corresponding results of simulation are tabulated in column 5 and 6. The measurements are stable under the same environmental condition. Significant figure is tenth here and standard deviation that marked as 0 represent highly stable experimental outcome. However, additional digit is added to the Std (standard deviation) for a better discrimination.

Table 2: Results of the experiments. Prot 1 denotes the prototype of {15.0, 9.0} mm height, while Prot 2 the prototype of {8.0, 5.0} mm height.

t_{bom} (°C)	t_{amb} (°C)	Mean (°C)		Simulation result (°C)		Std (°C)	
		Prot 1	Prot 2	Prot 1	Prot 2	Prot 1	Prot 2
36.0	27.6	35.2	35.3	35.4	35.6	0.00	0.00
37.0	28.5	36.5	36.6	36.3	36.6	0.06	0.01
38.0	28.5	37.4	37.5	37.2	37.5	0.15	0.00

4 DISCUSSION

In the numeric study phase, mesh qualities and the material values would affect the accuracy and simulation result greatly. In this study, the quality of mesh was guaranteed by the COMSOL Multiphysics software and the related physical parameters were extracted from the COMSOL material library. However, these parameters may not match the real

materials used perfectly, thus these differences could be considered as a reason for the deviation between simulations and experiments.

From the results of the simulations, two considerations on the thermometer's configuration should be given. One is that the height could not be decreased arbitrarily to ultra-thin level, says 1 mm, which will be very difficult to fabricate. Another one is the radius. We intend to maintain the miniature configuration and try to attain equal accuracy by reducing the height only. That is the reason why the radius of prototypes is kept unchanged.

The experiments were carried out under the laboratory environment, where the ambient temperature was regulated by central-air conditioning at about 28.0 °C. However, during the experiment, the ambient temperature couldn't be regulated at a constant value, which is the major limitation of these experiments. This limitation can also be considered as another reason for the deviation between simulations and experiments. However, the insight that DHF thermometer will benefit from a thinner design can be obtained. To obtain a more precise comparison, the experiment should be operated inside a thermostatic room, because that the performance of the thermometer is prone to be affected by the ambient temperature according to (Huang and Chen, 2010). What is more, in view of this disadvantage, an important direction of the next step of improvement should be the mitigation of the effect brought about by the environment.

The geometrical parameters that we adopted to fabricate here are only a subset of the parameters used in the simulations. The thicker one is of the similar configuration as the initial prototype of DHF method, while the thinner one is a product balancing the implementability and accuracy. To further elevate its accuracy, consideration except for the geometrical parameters should also be given, e.g., the arrangement of a urethane sponge to cover the thermometer. Of course, we could try to enlarge the radius to get a more satisfactory performance if only its size cause no obstruction to practical application.

5 CONCLUSIONS

We constructed 3D finite element models to carry out an overall numeric study of the geometrical parameters' effect on the performance of the DHF thermometer. According to the numeric results, we designed and fabricated prototypes and an experimental system. Results from both numeric and experiment studies show that to lower the height and enlarger the radius of the thermometer will improve its performance. Thermometer of 22.0 mm radius can acquire satisfactory accuracy with error less than 0.5 °C when height is 8.0 mm or less.

ACKNOWLEDGEMENTS

REFERENCES

Baehr, E. K., Revelle, W., and Eastman, C. I., 2000. Individual differences in the phase and amplitude of the human circadian temperature rhythm: with an emphasis on morningness-eveningness, *Journal of sleep research*, 9(2), pp. 117-27.

Bjoryatn, B., and Pallesen, S., 2009. A practical approach to circadian rhythm sleep disorders, *Sleep medicine reviews*, 13(1), pp. 47-60.

Fox, R. H., and Solman, A. J., 1971. A new technique for monitoring the deep body temperature in man from the intact skin surface, *J Physiol*, 212, pp. 8-10.

Gunga, H. C., Sandsund, M., Reinertsen, R. E., Sattler, F., and Koch, J., 2008. A non-invasive device to continuously determine heat strain in humans, *Journal of Thermal Biology*, 33(5), pp. 297-307.

Huang, M., and Chen, W., 2010. Theoretical simulation of the dual-heat-flux method in deep body temperature measurements, *Proceeding of IEEE EMBC 2010*, 2010, pp. 561-64.

Huang, M., Chen, W., Kitamura, K., Nemoto, T., and Tamura, T., 2013. Improvement of the Dual-heat-flux Method for Deep Body Temperature Measurement Based on a Finite Element Model, *Proceeding of IEEE EMBC 2013*, 2013, pp. 1202-05.

Kimberger, O., Thell, R., Schuh, M., Koch, J., Sessler, D. I., and Kurz, A., 2009. Accuracy and precision of a novel non-invasive core thermometer," British journal of anaesthesia. *British journal of anaesthesia.* 103(2), pp. 226-31.

Kitamura, K., Zhu, X., Chen, W., and Nemoto, T., 2010. Development of a new method for the noninvasive measurement of deep body temperature without a heater, *Medical Engineering & Physics*, 32(1), pp. 1-6.

NICE, 2008. http://www.nice.org.uk/CG065.